Optics Communications 356 (2015) 620–627

Contents lists available at ScienceDirect

Optics Communications

journal homepage: www.elsevier.com/locate/optcom

The performance of heterodyne detection system for partially coherent beams in turbulent atmosphere

Li Chengqiang [a,b,*], Wang Tingfeng [a], Zhang Heyong [a], Xie Jingjiang [c], Liu Lisheng [a], Zhao Shuai [a], Guo Jin [a]

[a] State Key Laboratory of Laser Interaction with Matter, Changchun Institute of Optics, Fine Mechanics and Physics, Chinese Academy of Sciences, Changchun 130033, China
[b] University of Chinese Academy of Sciences, Beijing 100049, China
[c] Key Laboratory of Optical System Advanced Manufacturing Technology, Changchun Institute of Optics, Fine Mechanics and Physics, Chinese Academy of Sciences, Changchun 130033, China

ARTICLE INFO

Article history:
Received 28 May 2015
Received in revised form
21 July 2015
Accepted 25 August 2015

Keywords:
Detection
Heterodyne
Atmospheric turbulence
Laser beam transmission

ABSTRACT

The performance of heterodyne system is discussed for partially coherent beams in turbulent atmosphere by introducing turbulence spectrum of refractive-index fluctuations. Several analytic formulae for the heterodyne detection system using the partially coherent Gaussian Schell-model beam are presented. Based on Tatarskii spectrum model, some numerical results are given for the variation in the heterodyne efficiency with the misalignment angle, detector diameter, turbulence conditions, and parameters of the overlapping beams. According to the numerical results, we find that the turbulent atmosphere degrades the heterodyne efficiency significantly, and the variation in heterodyne efficiency is even slower against the misalignment angle in turbulence. For the deterministic received signal and the detector, the performance of the heterodyne detection can be adjusted by controlling the local oscillator signal parameters.

1. Introduction

Heterodyne detection is a widely used technique in the microwave region. Heterodyne technique has been extended to the optical regions owing to its noise-reduction capabilities and high spectral resolution in comparison with incoherent (direct) detection [1]. Heterodyne (coherent) detection is a more powerful detection technique for long-range and weak signal detections [2]. At the same time, heterodyne detection system needs more stringent technical requirements than incoherent detection does. In order to ensure the performance of optical heterodyne detection system, the wavefront, amplitude and polarization of the local oscillator (LO) and signal beams should be matched strictly [3–5]. The wavefront alignment between signal and local oscillator beams required for effective optical heterodyne is treated by Siegman, which is summarized in the "antenna theorem" for optical heterodyne [6]. In order to obtain the high performance, it is necessary to match the locally generated beam parameters with the received signal beam parameters on the detector [7]. Heterodyne efficiency of the optical coherent detection system reflects the matching degree of phase and amplitude between the local oscillator and received signal beams [8]. The heterodyne efficiency is considered as a measurement to evaluate the performance of the heterodyne technique. It may also be used to quantify the potential mismatch between the locally generated signal and the received one [9]. The mismatch directly reduces the signal-to-noise ratio (*SNR*) of the detection system.

The performance of the heterodyne system for spatially fully coherent signals has been investigated in previous works. The effect of atmospheric turbulence on the heterodyne performance has been studied for coherent laser radar systems [10,11]. General expressions are derived for the *SNR* of a coherent detection system in terms of the deterministic received signal and local oscillator fields including the parameters of detector [12]. Tanaka and Saga considered the maximum heterodyne efficiency for an optical heterodyne detection system in the presence of background radiation [13]. The performance of an optical heterodyne detection system with aberrations is studied theoretically and experimentally [14,15].

However, most of the physically realizable optical sources radiate randomly due to the inhomogeneity in resonant cavity and the characteristics of spontaneous emission of the atoms [16,17]. On the other hand, the phase front will become chaotic after

* Corresponding author at: State Key Laboratory of Laser Interaction with Matter, Changchun Institute of Optics, Fine Mechanics and Physics, Chinese Academy of Sciences, Changchun 130033, China.
E-mail address: hitwhfeixiang@msn.cn (L. Chengqiang).

http://dx.doi.org/10.1016/j.optcom.2015.08.075
0030-4018/

coherent radiation propagating through turbulent media. These reasons result in partially coherent radiation [18]. Hence, the performance of an optical heterodyne system for partially coherent beams should be treated thoroughly. Optical heterodyne detection of partially coherent cross-spectrally pure radiation is considered by Chiou [1]. Tanaka et al. studied the heterodyne efficiency for partially coherent optical signals [19]. The performance of a misaligned heterodyne detection system for partially coherent beams is treated by Salem and Rolland [20]. However, Salem and Rolland did not address the effects of atmospheric turbulence. The effects of turbulent atmosphere on the performance of heterodyne system cannot be ignored in practical applications. Based on the atmospheric coherence length or Fried parameter, Ren et al. discussed the performance of coherent free-space optical communication system [21]. It is feasible to employ various models of the power spectrum for atmospheric turbulence as an effective way to discuss the effects of atmosphere on the heterodyne system. However, the similar works have not been described in the previous treatments.

In this paper, the effects of turbulent atmosphere on the performance of heterodyne system are studied for partially coherent beams based on the turbulence spectrum of the refractive-index fluctuations [22]. General expressions that include turbulence spectrum for the heterodyne performance for mixing two partially coherent and quasi-monochromatic beams on a detector surface are obtained. The Tatarskii spectrum model is employed to investigate the effects of turbulent atmosphere on the performance of optical heterodyne detection system in this study. The Tatarskii spectrum improves the agreement between theory and experimental measurements by truncating the spectrum at high wave numbers in the presence of atmospheric turbulence [22]. For different cases, some numerical results are presented to show the performance of heterodyne system with different beam parameters under the influence of atmospheric turbulence. The effect of the misalignment angle on the heterodyne efficiency in turbulence is also investigated. Additionally, the joint effects of different conditions will be discussed in detail in the following.

2. Heterodyne performance of partially coherent beam

Although the local oscillator is typically coherent, we consider the local oscillator being partially coherent to obtain an expression that is applicable to the most general cases for the heterodyne efficiency including the coherence properties of the light source. Let us consider two quasi-monochromatic and partially coherent beams propagating to a detector located at $z=0$ plane in a Cartesian coordinate system. We further assume that the propagation direction of the local oscillator beam is perpendicular to the detector surface but with a misalignment angle θ between its direction and the propagation direction of received signal as shown in Fig. 1.

The instantaneous field of both signals at the detector surface

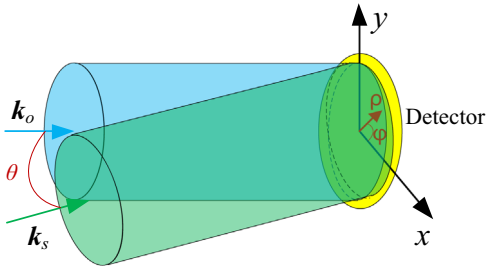

Fig. 1. The model of mixing two beams on a detector located at $z=0$ plane.

can be expressed as

$$U_o(\boldsymbol{\rho}, t) = U_o(\boldsymbol{\rho})e^{i\omega_o t} \tag{1}$$

$$U_s(\boldsymbol{\rho}, t) = U_s(\boldsymbol{\rho})e^{i\omega_s t - i\mathbf{k}\cdot\boldsymbol{\rho}} \tag{2}$$

where ω_o and ω_s are the central angular frequencies of the signals and $\mathbf{k}$ is the wave vector of the received signal. The subscripts o, s denote the locally generated signal and received signal respectively. Based on the model of heterodyne detection [23], the detected intermediate frequency (IF) power can be given by the expression [20]

$$P_{IF} = \iint\iint 2\Re(\boldsymbol{\rho}_1)\Re(\boldsymbol{\rho}_2)\mathrm{Re}\left[\Gamma_o(\boldsymbol{\rho}_1,\boldsymbol{\rho}_2)\Gamma_s^*(\boldsymbol{\rho}_1,\boldsymbol{\rho}_2)e^{i\mathbf{k}\cdot\boldsymbol{\rho}_1 - i\mathbf{k}\cdot\boldsymbol{\rho}_2}\right]d^2\boldsymbol{\rho}_1 d^2\boldsymbol{\rho}_2 \tag{3}$$

where $\Re(\boldsymbol{\rho})=e\eta(\boldsymbol{\rho})/h\nu$ is the detector responsivity at point $\boldsymbol{\rho}$, $\eta(\boldsymbol{\rho})$ is the quantum efficiency, e is the electronic charge, $h\nu$ is the photo energy, and $\Gamma_o(\boldsymbol{\rho}_1, \boldsymbol{\rho}_2)$ and $\Gamma_s(\boldsymbol{\rho}_1, \boldsymbol{\rho}_2)$ are the mutual coherence functions of the received and LO beams on the detector surface respectively [24]. The IF power is the useful part of the output of detector, and the other part of the output is random noise. The noise sources are of two types: those which depend on the power of local oscillator beam and those which are independent of the locally generated beam. Commonly, the standard shot-noise power of local oscillator field exceeds the other noises in the detection system and eventually becomes the dominant noise source. Assuming that the detector is operating at the shot-noise limit, the noise equivalent power could be defined as the shot-noise power of the local oscillator beam. The shot-noise power of the local oscillator beam is given by [23]

$$P_n = 2eB\iint \Re(\boldsymbol{\rho})\Gamma_o(\boldsymbol{\rho},\boldsymbol{\rho})d^2\boldsymbol{\rho} \tag{4}$$

where B is the receiver bandwidth of the detector. Using the results of the IF power and shot-noise power, it is easy to derive the expression of SNR as [20,25]

$$SNR = \frac{\iint\iint 2\Re(\boldsymbol{\rho}_1)\Re(\boldsymbol{\rho}_2)\mathrm{Re}\left[\Gamma_o(\boldsymbol{\rho}_1,\boldsymbol{\rho}_2)\Gamma_s^*(\boldsymbol{\rho}_1,\boldsymbol{\rho}_2)e^{i\mathbf{k}\cdot\boldsymbol{\rho}_1 - i\mathbf{k}\cdot\boldsymbol{\rho}_2}\right]d^2\boldsymbol{\rho}_1 d^2\boldsymbol{\rho}_2}{2eB\iint \Re(\boldsymbol{\rho})\Gamma_o(\boldsymbol{\rho},\boldsymbol{\rho})d^2\boldsymbol{\rho}} \tag{5}$$

Assuming that the detector responsivity $\Re$ is uniform across the detector surface and considering that those parameters do not affect the SNR variation, Eq. (5) can be further simplified as

$$SNR^+ = \frac{\iint\iint \mathrm{Re}\left[\Gamma_o(\boldsymbol{\rho}_1,\boldsymbol{\rho}_2)\Gamma_s^*(\boldsymbol{\rho}_1,\boldsymbol{\rho}_2)e^{i\mathbf{k}\cdot\boldsymbol{\rho}_1 - i\mathbf{k}\cdot\boldsymbol{\rho}_2}\right]d^2\boldsymbol{\rho}_1 d^2\boldsymbol{\rho}_2}{\iint\Gamma_o(\boldsymbol{\rho},\boldsymbol{\rho})d^2\boldsymbol{\rho}} \tag{6}$$

It is easy to see that the SNR^+ is a normalized SNR, $SNR^+ = SNReB/\Re$. The SNR^+ variation depends on the beam parameters and detector diameter. Another useful measurement of heterodyne performance is the dimensionless heterodyne efficiency η_h, which measures the loss in coherent power when the received and LO field are not perfectly matched. The heterodyne efficiency for random fields is defined in an analogous manner to the case of deterministic fields, i.e. [20]

$$\eta_h = \frac{\iint\iint \Re(\boldsymbol{\rho}_1)\Re(\boldsymbol{\rho}_2)\mathrm{Re}\left[\Gamma_o(\boldsymbol{\rho}_1,\boldsymbol{\rho}_2)\Gamma_s^*(\boldsymbol{\rho}_1,\boldsymbol{\rho}_2)e^{i\mathbf{k}\cdot\boldsymbol{\rho}_1 - i\mathbf{k}\cdot\boldsymbol{\rho}_2}\right]d^2\boldsymbol{\rho}_1 d^2\boldsymbol{\rho}_2}{\iint\Re(\boldsymbol{\rho})\Gamma_o(\boldsymbol{\rho},\boldsymbol{\rho})d^2\boldsymbol{\rho}\iint\Re(\boldsymbol{\rho})\Gamma_s(\boldsymbol{\rho},\boldsymbol{\rho})d^2\boldsymbol{\rho}} \tag{7}$$

Under the assumption that the detector responsivity $\Re$ is uniform across the detector surface, the heterodyne efficiency in this case can be expressed as

$$\eta_h = \frac{\iint\iint \mathrm{Re}\left[\Gamma_o(\boldsymbol{\rho}_1,\boldsymbol{\rho}_2)\Gamma_s^*(\boldsymbol{\rho}_1,\boldsymbol{\rho}_2)e^{i\mathbf{k}\cdot\boldsymbol{\rho}_1 - i\mathbf{k}\cdot\boldsymbol{\rho}_2}\right]d^2\boldsymbol{\rho}_1 d^2\boldsymbol{\rho}_2}{\iint\Gamma_o(\boldsymbol{\rho},\boldsymbol{\rho})d^2\boldsymbol{\rho}\iint\Gamma_s(\boldsymbol{\rho},\boldsymbol{\rho})d^2\boldsymbol{\rho}} \tag{8}$$

Using Eqs. (6) and (8), one can express the SNR^+ of the

detection system in terms of the heterodyne efficiency as

$$SNR^{+} = \eta_h \iint \Gamma_s(\boldsymbol{\rho}, \boldsymbol{\rho}) d^2\boldsymbol{\rho} \tag{9}$$

It is evident from Eq. (16) that the SNR^{+} is in direct proportion to the heterodyne efficiency for the deterministic received signal.

Eqs. (6) and (8) are the basic expressions for partially coherent detection in this paper. In the following we are concerned with the performance of heterodyne detection for partially coherent beams in presence of atmospheric turbulence. Considering two partially coherent beams radiating from Gaussian Schell-model (GSM) source propagating to the detector, the mutual coherence function of GSM source is expressed as [24]

$$\Gamma_\alpha^{(0)}(\boldsymbol{r}_1, \boldsymbol{r}_2) = I_\alpha \exp\left[-\frac{\boldsymbol{r}_1^2 + \boldsymbol{r}_2^2}{w_\alpha^2} - \frac{(\boldsymbol{r}_1 - \boldsymbol{r}_2)^2}{2\delta_\alpha^2} \right], (\alpha = o, s) \tag{10}$$

where w_α is the intensity width of the source, δ_α is the coherence width, or transverse coherence length, of the source, and I_α is the intensity of the source. As mentioned before, the subscripts o, s denote the locally generated and received signal respectively. Assuming that the fields radiating from the source propagation along the positive z-axis, it is easy to obtain the mutual coherence function of the fields according to the extended Huygens–Fresnel principle [22]. Considering the effects of turbulent atmosphere, the expression for mutual coherence function can be given as

$$\Gamma_\alpha(\boldsymbol{\rho}_1, \boldsymbol{\rho}_2, z_\alpha) = \left(\frac{k}{2\pi z_\alpha}\right)^2 \iint d^2\boldsymbol{r}_1 \iint d^2\boldsymbol{r}_2 \Gamma_\alpha^{(0)}(\boldsymbol{r}_1, \boldsymbol{r}_2) \exp\left[-ik\frac{(\boldsymbol{\rho}_1 - \boldsymbol{r}_1)^2 - (\boldsymbol{\rho}_2 - \boldsymbol{r}_2)^2}{2z_\alpha} \right] \times \left\langle \exp\left[\psi^*(\boldsymbol{\rho}_1, \boldsymbol{r}_1, z_\alpha) + \psi(\boldsymbol{\rho}_2, \boldsymbol{r}_2, z_\alpha)\right] \right\rangle_m \tag{11}$$

where $k = 2\pi/\lambda$, λ is the wavelength, z_α is the propagation distance of the beams, ψ is the random part of complex phase of a spherical wave propagating in the turbulent medium from the point $(\boldsymbol{\rho},0)$ to the point $(\boldsymbol{r},z_\alpha)$, and $\langle \cdots \rangle_m$ denotes averaging over the ensemble of statistical realizations of the turbulent medium. The angular bracket that reflects the effect of turbulence can be approximated as [26]

$$\left\langle \exp\left[\psi^*(\boldsymbol{\rho}_1, \boldsymbol{r}_1, z_\alpha) + \psi(\boldsymbol{\rho}_2, \boldsymbol{r}_2, z_\alpha)\right] \right\rangle_m \approx \exp\left\{ -M\left[(\boldsymbol{r}_1 - \boldsymbol{r}_2)^2 + (\boldsymbol{r}_1 - \boldsymbol{r}_2)(\boldsymbol{\rho}_1 - \boldsymbol{\rho}_2) + (\boldsymbol{\rho}_1 - \boldsymbol{\rho}_2)^2 \right] \right\} \tag{12}$$

where

$$M = \frac{1}{3}\pi^2 k^2 z_\alpha \int_0^\infty \kappa^3 \Phi_n(\kappa) d\kappa \tag{13}$$

Here $\Phi_n(\kappa)$ is the spectrum of the refractive-index fluctuations. There are different spectrum models for the refractive-index fluctuations, in view of the characteristics of spectrum models and mathematical complexity, the Tatarskii model is chosen [22]

$$\Phi_n(\kappa) = 0.033 C_n^2 \kappa^{-11/3} \exp\left(-\frac{\kappa^2}{\kappa_m^2}\right), \ (\kappa \gg 1/L_0, \kappa_m = 5.92/l_0) \tag{14}$$

where C_n^2 is known as the refractive-index structure parameter, κ is spatial frequency, l_0 is the inner scale of turbulence and L_0 the outer scale of turbulence. The inner scale l_0 can be few millimeters near the ground to a few centimeters high above the ground. Near the ground, L_0 is on the order of the height above ground, while high above the ground, it can be just tens to hundreds meters. Substituting Eqs. (10) and (12) into Eq. (11) and performing the inside integration yield

$$\Gamma_a(\rho_1, \rho_2, z_\alpha) = \frac{I_\alpha}{Q_\alpha} \exp[-H_\alpha(\rho_1 - \rho_2)^2] \exp[-\frac{1}{2w_\alpha^2 Q_\alpha}(\rho_1 + \rho_2)^2] \times \exp[-ikT_\alpha(\rho_1^2 - \rho_2^2)] \tag{15}$$

where

$$\frac{1}{\theta_\alpha^2} = \frac{1}{w_\alpha^2} + \frac{1}{\delta_\alpha^2}, H_a = \frac{1}{2\theta_\alpha^2 Q_\alpha} + \frac{2M}{Q_\alpha} + M - \frac{2z_\alpha^2 M^2}{k^2 w_\alpha^2 Q_\alpha}$$
$$T_a = \frac{6z_\alpha M\theta_\alpha^2 + 2z_\alpha}{k^2 w_\alpha^2 Q_\alpha \theta_\alpha^2}, Q_\alpha = 1 + \frac{4z_\alpha^2}{k^2 w_\alpha^2 \theta_\alpha^2} + \frac{8z_\alpha^2 M}{k^2 w_\alpha^2} \tag{16}$$

It is evident that when $z_\alpha = 0$, Eq. (15) reduces to the form given by Eq. (10). Now the analysis of the heterodyne performance for partially coherent beams can be performed by using the results in Eq. (15). It is easy to obtain from Fig. 1 that $\boldsymbol{k\rho} = k\rho \sin\theta \cos\varphi$. Under the assumption that both the LO beam and the received beam on the detector surface can be expressed by the analytic forms given in Eq.(15), substituting Eq. (15) into Eq. (3) and converting to polar coordinates ρ and θ, the expression for the IF power can be expressed as

$$P_{IF} = 2\Re^2 \int_0^{2\pi} \int_0^{2\pi} \int_0^{D/2} \int_0^{D/2} \rho_1\rho_2 \, \mathrm{Re}\left\{ \frac{I_o}{Q_o} \exp\left[-H_o(\rho_1 - \rho_2)^2 \right] \exp\left[-\frac{1}{2w_o^2 Q_o}(\rho_1 + \rho_2)^2 \right] \times \exp\left[-ikT_o(\rho_1^2 - \rho_2^2) \right] \frac{I_s}{Q_s} \exp\left[-H_s(\rho_1 - \rho_2)^2 \right] \exp\left[ikT_s(\rho_1^2 - \rho_2^2) \right] \times \exp\left[-\frac{1}{2w_s^2 Q_s}(\rho_1 + \rho_2)^2 \right] e^{ik\rho_1 \sin\theta \cos\varphi_1 - ik\rho_2 \sin\theta \cos\varphi_2} \right\} d\rho_1 d\rho_2 d\varphi_1 d\varphi_2 \tag{17}$$

where the symbol D is the hard aperture diameter of the detector. In order to simplify the integration, it is reasonable to use a Gaussian limiting aperture, or soft aperture, to replace the hard aperture. The soft aperture radius W relates to a hard aperture diameter D according to $D^2 = 8W^2$ [22,27]. By using the soft aperture approximation, the Eq. (17) becomes

$$P_{IF} = 2\Re^2 \int_0^{2\pi} \int_0^{2\pi} \int_0^{\infty} \int_0^{\infty} \rho_1\rho_2 \, \mathrm{Re}\left\{ \frac{I_o}{Q_o} \exp\left[-H_o(\rho_1 - \rho_2)^2 \right] \exp\left[-\frac{1}{2w_o^2 Q_o}(\rho_1 + \rho_2)^2 \right] \times \exp\left[-ikT_o\left(\rho_1^2 - \rho_2^2\right) \right] \frac{I_s}{Q_s} \exp\left[-H_s(\rho_1 - \rho_2)^2 \right] \exp\left[-\frac{1}{2w_s^2 Q_s}(\rho_1 + \rho_2)^2 \right] \times \exp\left[ikT_s\left(\rho_1^2 - \rho_2^2\right) \right] e^{ik\rho_1 \sin\theta \cos\varphi_1 - ik\rho_2 \sin\theta \cos\varphi_2} \exp\left[-\frac{\rho_1^2 + \rho_2^2}{W^2} \right] \right\} d\rho_1 d\rho_2 d\varphi_1 d\varphi_2 \tag{18}$$

The above integration is performed analytically as shown in detail in Appendix A. According to the results obtained in Appendix A, it is easy to write the expression of SNR^{+} as

$$SNR^{+} = \frac{\pi I_s[2W^2 + w_o^2 Q_o]}{W^2 w_o^2 Q_o Q_s (g^2 + s^2 - q^2)} \exp\left[\frac{q - g}{2(g^2 + s^2 - q^2)} k^2 \sin^2\theta\right] \tag{19}$$

Similarly, the heterodyne efficiency η_h is given as

$$\eta_h = \frac{[2W^2 + w_o^2 Q_o][2W^2 + w_s^2 Q_s]}{W^4 w_o^2 w_s^2 Q_o Q_s (g^2 + s^2 - q^2)} \exp\left[\frac{q - g}{2(g^2 + s^2 - q^2)} k^2 \sin^2\theta\right] \tag{20}$$

Eqs. (19) and (20) are the main formulae in this paper. In comparison to the previous reports, the correctness of the derivations can be proven by setting the turbulence intensity $C_n^2 = 0$. From Eqs. (19) and (20), it is easy to see that the performance of heterodyne system not only depends on the parameters of the received and locally generated beams, but also is governed by the effect of atmospheric turbulence and misalignment angle θ of two overlapped signals on the detector surface.

3. Numerical results

In this section, the performance of heterodyne detection system is studied by numerical simulation, and the results are illustrated graphically. According to Eqs. (19) and (20) given in foregoing section, the heterodyne efficiency is determined by detector diameter, turbulence conditions, misalignment angle θ, and the parameters of locally generated signal and received signal. Firstly, we set some parameters globally. In the listing, the inner scale is l_0 =5 mm, and the wavelength of light source is λ=532 nm.

Let us begin with studying the variation of the heterodyne efficiency with the detector diameter for several cases. Assuming the same parameters for the received signal and varying the parameters of locally generated signal, the effects of local oscillator beam parameters and detector diameter on the heterodyne efficiency η_h is shown in Fig. 2. Fig. 2(a) illustrates the effect of the beam width of local oscillator signal on the heterodyne efficiency versus the detector diameter. It is easy to see that the matching beam widths of the two overlapped signals leads to higher heterodyne efficiency, and increasing the detector diameter degrades the heterodyne efficiency. Hence, in order to improve the heterodyne efficiency, the beam width of the two overlapped signals should keep matching. Meanwhile, choosing the appropriate detector size is helpful to obtain higher heterodyne efficiency. In Fig. 2(b), we show the variation of the heterodyne efficiency against detector diameter with the misalignment angle θ=0.1 mrad. One can find that the angular shift between the two signals generally degrades the heterodyne efficiency. By comparison, one can find that the heterodyne efficiency η_h keeps higher as the beam width w_o=3 mm in Fig. 2 (a) while η_h is higher in Fig. 2(b) as w_o=2 mm. The difference is caused by the misalignment angle θ, and the physical interpretation of this phenomenon is that the diffraction of beam is different under the misalignment angle θ.

Fig. 3(a) shows the variation of the heterodyne efficiency with the intensity width w_o of the local oscillator signal for several values of the intensity width w_s of the received signal. In this case, by increasing the intensity width w_s and reaching the matching status with respect to the intensity width of local oscillator signal, one can potentially obtain the maximum heterodyne efficiency. For the deterministic detector diameter, it is necessary to keep the received signal matching with the LO signal strictly for high heterodyne efficiency. But if the intensity width of the both beams is greater or equal to the detector diameter, with a slight mismatch between the LO beam and the received beam, the efficiency η_h can still remain at a high level. Actually, the received beam may exist jitters on the detector surface caused by turbulent atmosphere. Generally, in order to keep higher heterodyne efficiency, the beam width of the local oscillator signal should be appreciably larger than the received signal's to ensure the overlap of the two beams. Fig. 3(b) shows the effect of the coherence widths of the both signals on the heterodyne efficiency. For the fixed detector diameter, increasing the coherence width δ_s of the received signal has minimal effect on the heterodyne efficiency for the small coherence width δ_o of local oscillator signal. But the variation of the heterodyne efficiency with δ_s is evident as δ_o is big enough. With the limitations of detector diameter and intensity widths of the signals, the heterodyne efficiency changes little with the increase of δ_s when δ_s is up to a certain level. The matching status of the both signals leads to the high mixing efficiency under certain detector diameter.

Fig. 4 illustrates the effects of turbulence on the heterodyne efficiency versus the detector diameter with or without the misalignment angle. In Fig. 4(a), we show the variation of heterodyne efficiency with the different turbulence conditions for the misalignment angle θ=0. It is evident that the heterodyne efficiency is monotonically decreasing with the turbulence intensity reflected by C_n^2. The results in Fig. 4(a) suggest that the effect of turbulence on the heterodyne efficiency is strong. Fig. 4(b) shows the effect of turbulence on the heterodyne efficiency with the misalignment angle θ=0.2 mrad. The heterodyne efficiency η_h decreases rapidly versus the detector diameter as the turbulence intensity enhances. For the stronger turbulence, one can find that the η_h drops steeply, and the change in heterodyne efficiency is more even slow against the detector diameter as the heterodyne efficiency η_h is at a low level. Fig. 4(c) shows the variation in η_h versus the turbulence intensity that characterized by C_n^2. As there is a mismatch between the LO signal and the received signal, the heterodyne efficiency η_h is decreased further.

Fig. 5 demonstrates the effects of misalignment angle on heterodyne efficiency for different cases. In Fig. 5(a), we plot the variation in heterodyne efficiency against the misalignment angle for the different intensity width w_s of the received signal. One can find that the peak of the efficiency curve varies with the change in the intensity width w_s. Increasing the intensity width can obtain a higher peak value. Meanwhile, the large beam width means a small scale of misalignment angle. The effect of detector diameter on heterodyne efficiency versus the misalignment angle without turbulence is shown in Fig. 5(b). The change in detector diameter has slight effect on the peak value of the heterodyne efficiency curve. But the width of peak is negatively related to the detector diameter. This phenomenon can be elucidated clearly by using the diffraction limit theory. The angle semibreadth of airy disk is negatively related to the detector diameter and proportional to the wavelength. Fig. 5(c) shows the effect of atmospheric turbulence

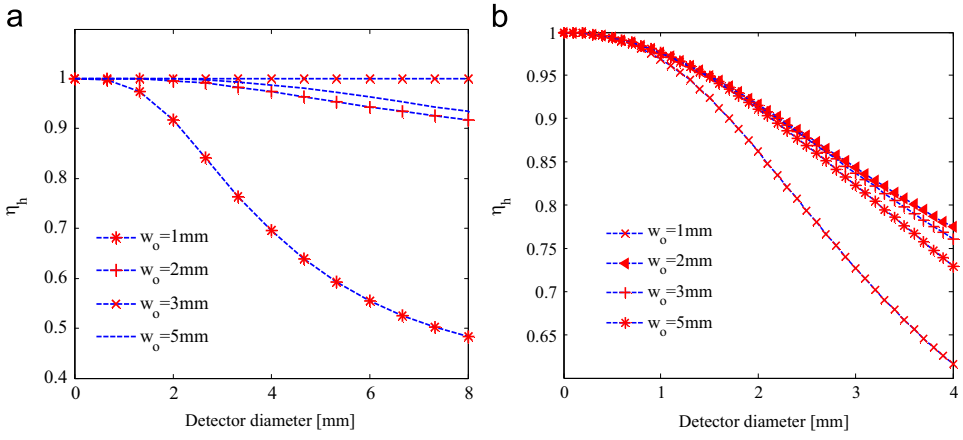

Fig. 2. Heterodyne efficiency versus the detector diameter for the different intensity widths of the local oscillator beams with or without the misalignment angle. (a) w_s=3 mm, δ_s=∞, δ_o=∞, z_o=0 m, z_s=0 m, θ=0 mrad, (b) w_s=3 mm, δ_s=∞, δ_o=∞, z_o=0 m, z_s=0 m, θ=0.1 mrad.

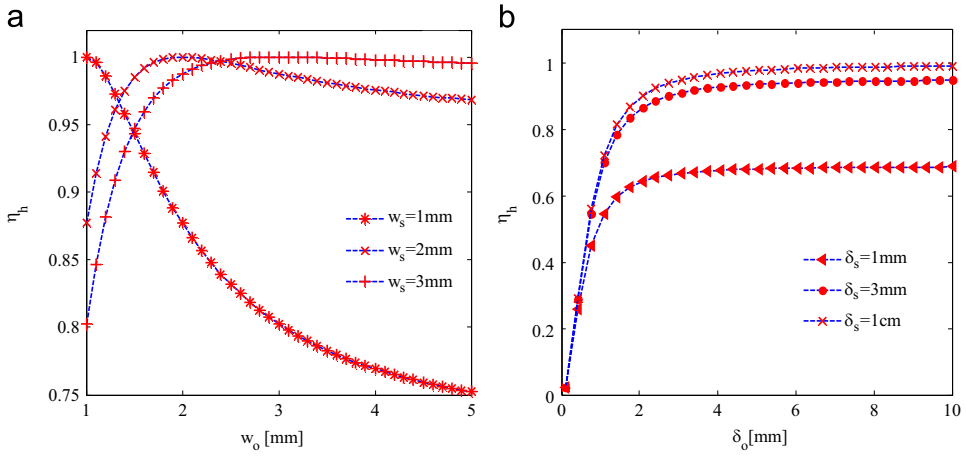

Fig. 3. The variation of the heterodyne efficiency with the parameters of the mixing beams. (a) z_o=0 m, z_s=0 m, δ_o=∞, δ_s=∞, D=3 mm, θ=0 mrad, (b) z_o=0 m, z_s=0 m, w_o=3 mm, w_s=3 mm, D=2 mm, θ=0 mrad.

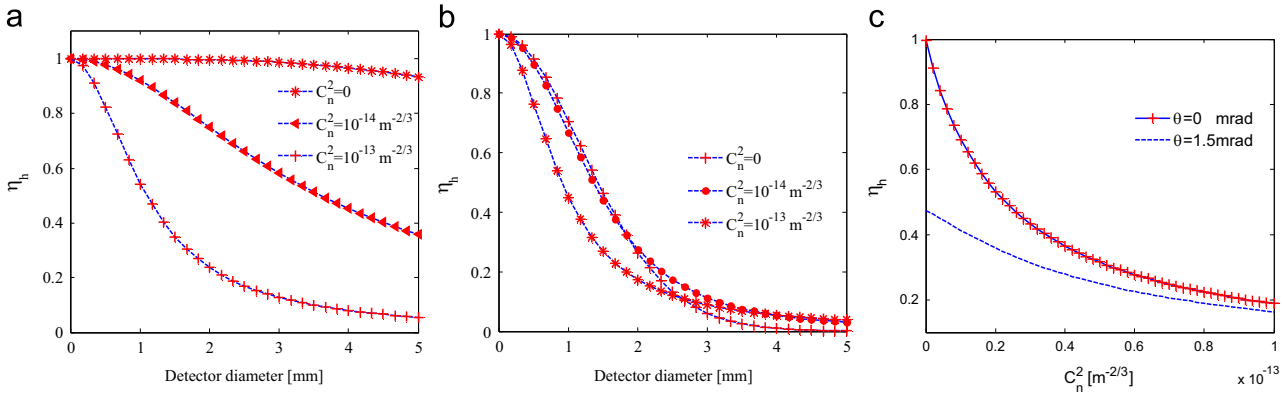

Fig. 4. The effect of turbulence on heterodyne efficiency with or without the misalignment angle, (a) z_s=10^5 m, z_o=0 m, w_s=3 mm, w_o=3 mm, δ_o=∞, δ_s=1, θ=0 mrad, (b) z_s=10^5 m, z_o=0 m, w_s=3 mm, w_o=3 mm, δ_o=∞, δ_s=1, θ=0.2 mrad, (c) z_s=10^5 m, z_o=0 m, w_s=3 mm, w_o=3 mm, δ_o=∞, δ_s=∞, D=2 mm, θ=0.15 mrad.

on the heterodyne efficiency. The curves reveal the negative correlation between turbulence intensity and the peak value. Increasing the turbulence intensity can obtain a wider peak, but the peak value decreases with turbulence intensity. Under the turbulence condition, the variation of the heterodyne efficiency with detector diameter is illustrated in Fig. 5(d). The entire curves become lower with the increase of detector diameter. It is observed from Fig. 5(d) that choosing an appropriate detector diameter is helpful to obtain a higher heterodyne efficiency.

4. Conclusion

Based on the turbulence spectrum of the refractive-index fluctuations, several analytic formulae have been derived to evaluate the performance of optical heterodyne detection system for partially coherent GSM beams with the misalignment angle between the local oscillator signal and received signal. According to the obtained expressions in Section 2, the Tatarskii spectrum model is chosen to perform numerical analysis. Based on the numerical results, the performance of heterodyne detection system for partially coherent beams in atmospheric turbulence is studied in detail. Under turbulence conditions, we demonstrate that the heterodyne efficiency can be adjusted by controlling the detector diameter, the misalignment angle and local oscillator beam parameters. For the deterministic received signal and the detector, the optimal values of the local oscillator signal parameters can be obtained easily. We show that the heterodyne efficiency for the partially coherent beams in turbulence is more stable with respect to the misalignment of the detection system.

Appendix A. Analytical forms for signal power

In this appendix, the analytic form of IF power is derived first. Using the relationship $\boldsymbol{\rho}_1\boldsymbol{\rho}_2=\rho_1\rho_2\cos(\varphi_1-\varphi_2)$ and rearranging the integration, Eq. (18) can be written as

$$P_{IF}=2\Re^2\int_0^{2\pi}\int_0^{2\pi}\int_0^{\infty}\int_0^{\infty}\rho_1\rho_2\frac{I_oI_s}{Q_oQ_s}\,\mathrm{Re}\Big\{\exp\big(-g\rho_1^2-g\rho_2^2\big)\exp\big[2q\rho_1\rho_2\cos(\varphi_1-\varphi_2)\big]\times\exp\big[ik(\rho_1\cos\varphi_1-\rho_2\cos\varphi_2)\sin\theta\big]\exp\big(is\rho_1^2-is\rho_2^2\big)\Big\}\,d\rho_1d\rho_2d\varphi_1d\varphi_2 \tag{21}$$

where

$$g=H_o+\frac{1}{2w_o^2Q_o}+H_s+\frac{1}{2w_s^2Q_s}+\frac{1}{W^2},\quad s=k\big[T_s-T_o\big]$$
$$q=H_o-\frac{1}{2w_o^2Q_o}+H_s-\frac{1}{2w_s^2Q_s} \tag{22}$$

In order to perform the integration over φ_1, Eq. (21) is simply rearranged as

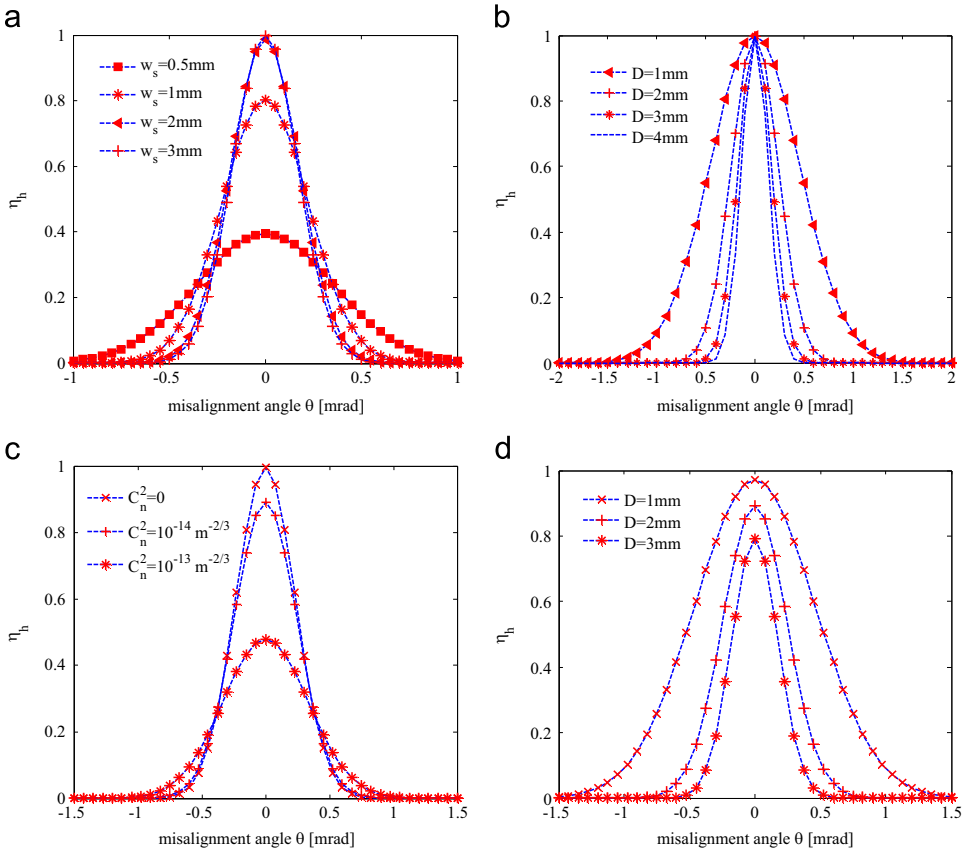

Fig.5. The variation of the heterodyne efficiency with the misalignment angle for different cases, (a) z_o=0 m, z_s=0 m, w_o=3 mm, δ_s=∞, δ_o=∞, D=3 mm, (b) z_o=0 m, z_s=0 m, w_o=3 mm, w_s=3 mm, δ_s=∞, δ_o=∞, (c) z_o=0 m, z_s=10^5 m, w_s=3 mm, w_o=3 mm, δ_s=0.5 mm, δ_o=∞, D=2 mm, (d) z_o=0 m, z_s=10^5 m, w_s=3 mm, w_o=3 mm, δ_s=0.5 mm, δ_o=∞, C_n^2=10^{-14} $m^{-2/3}$.

$$P_{IF} = 2\Re^2 \int_0^{2\pi}\int_0^{\infty}\int_0^{\infty} \rho_1\rho_2 \frac{I_oI_s}{Q_oQ_s}\,\mathrm{Re}\Big\{\exp\big(-g\rho_1^2-g\rho_2^2\big) \times \exp\big(is\rho_1^2-is\rho_2^2\big)\exp(-ik\rho_2\sin\theta\cos\varphi_2)d\rho_1d\rho_2d\varphi_2 \times \int_0^{2\pi}\exp(2q\rho_1\rho_2\cos\varphi_2\cos\varphi_1+2q\rho_1\rho_2\sin\varphi_2\sin\varphi_1) \times \exp\big[i(k\rho_1\sin\theta)\cos\varphi_1\big]d\varphi_1\Big\} \tag{23}$$

Using the identities written as formulas 3.937 in [28], it is easy to establish the identity given as

$$\int_0^{2\pi}\exp(p\cos x+q\sin x)\exp(ia\cos x)dx = 2\pi I_0\big(\sqrt{C+iD}\big),\ p^2+(a+q)^2>0 \tag{24}$$

where

$$C=p^2+q^2-a^2,\quad D=2ap \tag{25}$$

Employing the identity defined by Eq. (24), Eq. (23) becomes

$$P_{IF} = 4\pi\Re^2 \int_0^{2\pi}\int_0^{\infty}\int_0^{\infty} \rho_1\rho_2 \frac{I_oI_s}{Q_oQ_s}\,\mathrm{Re}\Big\{\exp\big(-g\rho_1^2-g\rho_2^2\big) \times \exp\big(is\rho_1^2-is\rho_2^2\big)\exp(-ik\rho_2\sin\theta\cos\varphi_2)d\rho_1d\rho_2d\varphi_2 \times I_0\Big(\sqrt{4q^2\rho_1^2\rho_2^2-k^2\rho_1^2\sin^2\theta+i4kq\rho_1^2\rho_2\sin\theta\cos\varphi_2}\Big)\Big\} \tag{26}$$

Here $I_\nu(\cdots)$ is the modified Bessel function of order ν. By using the identity [29]

$$I_\nu(\varpi)\begin{matrix}\cos\\ \sin\end{matrix}\nu\psi = \sum_{m=-\infty}^{\infty}(-1)^m I_{\nu+m}(Z)I_m(z)\begin{matrix}\cos\\ \sin\end{matrix}m\phi$$
$$\varpi=\sqrt{Z^2+z^2-2Zz\cos\phi} \tag{27}$$

Eq. (26) can be written as

$$P_{IF} = 4\pi\Re^2 \int_0^{2\pi}\int_0^{\infty}\int_0^{\infty} \rho_1\rho_2 \frac{I_oI_s}{Q_oQ_s}\,\mathrm{Re}\Big\{\exp\big(-g\rho_1^2-g\rho_2^2\big) \times \exp\big(is\rho_1^2-is\rho_2^2\big)\exp(-ik\rho_2\sin\theta\cos\varphi_2)d\rho_1d\rho_2d\varphi_2 \times \sum_{m=-\infty}^{\infty}(-1)^m I_m(2q\rho_1\rho_2)I_m(ik\rho_1\sin\theta)\cos\big[m(\varphi_2-\pi)\big]\Big\} \tag{28}$$

Rearranging the terms in Eq. (28) leads to

$$P_{IF} = 4\pi\Re^2 \int_0^{\infty}\int_0^{\infty} \rho_1\rho_2 \frac{I_oI_s}{Q_oQ_s}\,\mathrm{Re}\Big\{\exp\big(-g\rho_1^2-g\rho_2^2\big)\exp\big(is\rho_1^2-is\rho_2^2\big) \times \sum_{m=-\infty}^{\infty}(-1)^m\cos(m\pi)I_m(2q\rho_1\rho_2)I_m(ik\rho_1\sin\theta) \times \int_0^{2\pi}\exp(-ik\rho_2\sin\theta\cos\varphi_2)\cos(m\varphi_2)d\varphi_2\Big\}d\rho_1d\rho_2 \tag{29}$$

Using the identities written as formulae 3.715 in [28], it is not difficult to form the new identity given as

$$\int_0^{2\pi}\exp(iz\cos x)\cos lx\,dx = 2\pi(-1)^l\exp\Big(-i\frac{l\pi}{2}\Big)J_l(z) \tag{30}$$

where $J_l(\cdots)$ is Bessel function of the first kind of order l. Performing the integration over φ_2 by using the identity in Eq. (30) and rearranging yield

$$P_{IF} = 8\pi^2\Re^2 \int_0^\infty \int_0^\infty \rho_1\rho_2 \frac{I_o I_s}{Q_o Q_s} \mathrm{Re}\{\exp(-g\rho_1^2 - g\rho_2^2)\exp(is\rho_1^2 - is\rho_2^2) \times \sum_{m=-\infty}^{\infty} \exp(-i\frac{m\pi}{2})\cos(m\pi) I_m(2q\rho_1\rho_2) I_m(ik\rho_1 \sin\theta) \times J_m(-k\rho_2 \sin\theta)\} d\rho_1 d\rho_2 \quad (31)$$

Since [28,29]

$$I_m(z) = i^{-m} J_m(iz) \quad (32)$$

$$J_{-m}(x) = (-1)^m J_m(x) \quad (33)$$

$$I_{-m}(x) = I_m(x) \quad (34)$$

we have

$$P_{IF} = 8\pi^2\Re^2 \int_0^\infty \int_0^\infty \rho_1\rho_2 \frac{I_o I_s}{Q_o Q_s} \mathrm{Re}\{\exp(-g\rho_1^2 + is\rho_1^2)\exp(-g\rho_2^2 - is\rho_2^2) \times [I_0(2q\rho_1\rho_2) J_0(-k\rho_1 \sin\theta) J_0(-k\rho_2 \sin\theta) + \sum_{m=1}^{\infty} \cos(m\pi)(e^{-im\pi/2} i^{-m} + e^{im\pi/2} i^m) I_m(2q\rho_1\rho_2) \times J_m(-k\rho_1 \sin\theta) J_m(-k\rho_2 \sin\theta)]\} d\rho_1 d\rho_2 \quad (35)$$

Using Eq. (32) and the identity [28]

$$\int_0^\infty x e^{-\alpha x^2} J_\upsilon(\gamma x) I_\upsilon(\beta x) dx = \frac{1}{2\alpha} \exp\left(\frac{\beta^2 - \gamma^2}{4\alpha}\right) J_\upsilon\left(\frac{\beta\gamma}{2\alpha}\right),$$

$$(\mathrm{Re}\,\alpha > 0, \mathrm{Re}\,\upsilon > -1) \quad (36)$$

Performing the integration over ρ_1 and rearranging yield

$$P_{IF} = \frac{4\pi^2\Re^2}{g - is} \int_0^\infty \rho_2 \frac{I_o I_s}{Q_o Q_s} \mathrm{Re}\{\exp(-g\rho_2^2 - is\rho_2^2)\exp\left[\frac{4q^2\rho_2^2 - k^2 \sin^2\theta}{4(g - is)}\right] \times [J_0(-k\rho_2 \sin\theta) I_0\left(-\frac{kq\rho_2 \sin\theta}{s + ig}\right) + \sum_{m=1}^{\infty} \cos(m\pi) \times (e^{-im\pi/2} + (-1)^m e^{im\pi/2}) I_m\left(-\frac{kq\rho_2 \sin\theta}{s + ig}\right) J_m(-k\rho_2 \sin\theta)]\} d\rho_2 \quad (37)$$

Employing the identity given in Eq. (36) again, performing the integration over ρ_2 and rearranging the results by using Eq. (33) lead to

$$P_{IF} = 2\pi^2\Re^2 \frac{I_o I_s}{Q_o Q_s} \mathrm{Re}\left\{\frac{1}{t(g - is)} \exp\left[\frac{q^2 - (s + ig)^2}{4t(s + ig)^2} k^2 \sin^2\theta - \frac{1}{4(g - is)} k^2 \sin^2\theta\right] \sum_{m=-\infty}^{\infty} \cos(m\pi) \exp\left(-i\frac{m\pi}{2}\right) J_m\left(\frac{k^2 q \sin^2\theta}{2t(s + ig)}\right)\right\} \quad (38)$$

where

$$t = g + is - \frac{q^2}{(g - is)} \quad (39)$$

Using the series [29]

$$\cos(z \sin\theta) = J_0(z) + 2\sum_{n=1}^{\infty} J_{2n}(z)\cos 2n\theta$$

$$\sin(z \sin\theta) = 2\sum_{n=0}^{\infty} J_{2n+1}(z)\sin(2n + 1)\theta \quad (40)$$

we can establish a new formula given as

$$\sum_{m=-\infty}^{\infty} \cos(m\pi)\exp\left(-i\frac{m\pi}{2}\right) J_m(z) = e^{iz} \quad (41)$$

It is easy to deduce from Eqs. (38) and (41) that

$$P_{IF} = \frac{2\pi^2\Re^2 I_o I_s}{Q_o Q_s (g^2 + s^2 - q^2)} \exp[\frac{q - g}{2(g^2 + s^2 - q^2)} k^2 \sin^2\theta] \quad (42)$$

In the following, the key work is to perform the integration for the power of the local oscillator beam given as

$$P_o = \Re \iint \Gamma_o(\boldsymbol{\rho}, \boldsymbol{\rho}) d^2\boldsymbol{\rho} \quad (43)$$

Under the soft aperture approximation, substituting Eq. (15) into Eq. (43), converting to polar coordinates ρ and θ and using the identity [28]

$$\int_0^\infty x^m \exp(-\beta x^n) dx = \frac{\Gamma(\gamma)}{n\beta^\gamma}, \left[\gamma = \frac{m + 1}{n}, Re\beta > 0, \mathrm{Re}\, m > 0, Ren > 0\right] \quad (44)$$

we have

$$P_o = \frac{\pi\Re I_o W^2 w_o^2}{2W^2 + w_o^2 Q_o} \quad (45)$$

Similarly, the effective power of received signal is given as

$$P_s = \frac{\pi\Re I_s W^2 w_s^2}{2W^2 + w_s^2 Q_s} \quad (46)$$

References

[1] W. Chiou, Optical heterodyne detection of partially coherent radiation, in: 23rd Annual Technical Symposium (International Society for Optics and Photonics 1979), pp. 165–186.
[2] A.B. Gschwendtner, W.E. Keicher, Development of coherent laser radar at Lincoln Laboratory, Lincoln Lab. J. 12 (2000) 383–396.
[3] Q. Wang, C. Wang, T. Shang, Heterodyne efficiency of coherent detection with Guassian local-oscillator and Airy spot signal beam, Chin. J. Lasers 30 (2003) 183.
[4] Y. He, Phase matching of a heterodyne detection system, Chin. J. Lasers 10 (1997) 015.
[5] D. Sun, et al., Wave-front matching measurement in coherent CO_2 laser-radar, Appl. Opt. 31 (1992) 7647–7649.
[6] A. Siegman, The antenna properties of optical heterodyne receivers, Appl. Opt. 5 (1966) 1588–1594.
[7] S.C. Cohen, Heterodyne detection: phase front alignment, beam spot size, and detector uniformity, Appl. Opt. 14 (1975) 1953–1959.
[8] D.M. Chambers, Modeling of heterodyne efficiency for coherent laser radar in the presence of aberrations, Opt. Express 1 (1997) 60–67.
[9] R.G. Frehlich, Heterodyne efficiency for a coherent laser radar with diffuse or aerosol targets, J. Mod. Opt. 41 (1994) 2115–2129.
[10] M.S. Belen'kii, Effect of atmospheric turbulence on heterodyne lidar performance, Appl. Opt. 32 (1993) 5368–5372.
[11] K. Tanaka, N. Ohta, Effects of tilt and offset of signal field on heterodyne efficiency, Appl. Opt. 26 (1987) 627–632.
[12] D. Fink, Coherent detection signal-to-noise, Appl. Opt. 14 (1975) 689–690.
[13] K. Tanaka, N. Saga, Maximum heterodyne efficiency of optical heterodyne detection in the presence of background radiation, Appl. Opt. 23 (1984) 3901–3904.
[14] Q. Hu, et al., Investigation of spherical aberration effects on coherent lidar performance, Opt. Express 21 (2013) 25670–25676.
[15] D. Delautre, S. Breugnot, V. Laude, Measurement of the sensitivity of heterodyne detection to aberrations using a programmable liquid-crystal modulator, Opt. Commun. 160 (1999) 61–65.
[16] B.W. Tilma, et al., Recent advances in ultrafast semiconductor disk lasers, Light: Sci. Appl. 4 (2015) e310.
[17] A. Cui, et al., Directly patterned substrate-free plasmonic "nanograter" structures with unusual Fano resonances, Light: Sci. Appl. 4 (2015) e308.
[18] J. Wu, Propagation of a Gaussian-Schell beam through turbulent media, J. Mod. Opt. 37 (1990) 671–684.
[19] T. Tanaka, M. Taguchi, K. Tanaka, Heterodyne efficiency fo a partially coherent optical signal, Appl. Opt. 31 (1992) 5391–5394.
[20] M. Salem, J.P. Rolland, Heterodyne efficiency of a detection system for partially coherent beams, J. Opt. Soc. Am. A 27 (2010) 1111–1119.
[21] Y. Ren, et al., Heterodyne efficiency of a coherent free-space optical communication model through atmospheric turbulence, Appl. Opt. 51 (2012) 7246.
[22] L.C. Andrews, R.L. Phillips, Laser Beam Propagation Through Random Media, SPIE press, Bellingham, 2005.
[23] G.R. Osche, Optical Detection Theory for Laser Applications, Wiley, New York, 2002.

[24] L. Mandel, E. Wolf, Optical Coherence and Quantum Optics, Cambridge University Press, 1995.
[25] R.G. Frehlich, M.J. Kavaya, Coherent laser radar performance for general atmospheric refractive turbulence, Appl. Opt. 30 (1991) 5325–5352.
[26] C. Li, et al., Investigation on coherence characteristics of Gauss-Schell model beam propagating in atmospheric turbulence, Acta Phys. Sin. 62 (2013).
[27] L.C. Andrews, R.L. Phillips, C.Y. Hopen, Laser Beam Scintillation with Applications, SPIE press, Bellingham, 2001.
[28] A. Jeffrey, D. Zwillinger, Table of Integrals, Series, and Products, Academic Press, New York, 2007.
[29] G.N. Watson, A treatise on the theory of Bessel functions, Cambridge University Press, Cambridge, 1995.